

# 1 Mapping the probability of occurrence of invasive *Chromolaena odorata* in subtropical 2 forest gaps using environmental and remote sensing data

3  
4 Oupa E. Malahlela\* <sup>1,2</sup>, Moses A. Cho <sup>1,2</sup>, Onesimo Mutanga <sup>2</sup>

5 <sup>1</sup> Earth Observation Research Group, Natural Resources and Environment, Council for Scientific and Industrial  
6 Research, Pretoria 0001, South Africa

7 <sup>2</sup> Geography Department, University of KwaZulu-Natal, Pietermaritzburg Campus, Scottsville 3209, South  
8 Africa  
9

10 \*Corresponding author. Current address: P O Box 395, Pretoria, 0001, South Africa. Tel: +27 128412233.

11 Email address: [OMalahlela@csir.co.za](mailto:OMalahlela@csir.co.za)

12 M. A. Cho. Current address: P O Box 395, Pretoria, 0001, South Africa. Tel: +27 128413669. Email address:

13 [MCho@csir.co.za](mailto:MCho@csir.co.za)

14 O. Mutanga. Current address: P. Bag X01, Scottsville 3209, Pietermaritzburg, South Africa. Email address:

15 [MutangaO@ukzn.ac.za](mailto:MutangaO@ukzn.ac.za)  
16

## 17 Abstract

18 Globally, subtropical forests are rich in biodiversity. However, the native biodiversity of these forests  
19 is threatened by the presence of invasive species such as *Chromolaena odorata* which thrives in forest  
20 canopy gaps. Our study explored the utility of WorldView-2 data, an 8-band high resolution (2 m)  
21 imagery for mapping the probability of *C. odorata* occurrence (presence/absence) in canopy gaps of a  
22 subtropical forest patch, the Dukuduku Forest, South Africa. An integrated modelling approach  
23 involving the WorldView-2 bands and ancillary environmental data was also assessed. The results  
24 showed a higher performance of the environmental data only model (deviance or  $D^2 = 0.52$ ,  $p < 0.05$ ,  
25  $n = 77$ ) when compared to modelling with WorldView-2 vegetation indices such as the enhanced  
26 vegetation index (EVI), simple ratio indices (SRI) and red edge normalized difference vegetation  
27 index (NDVIR) ( $D^2 = 0.30$ ,  $p < 0.05$ ,  $n = 77$ ). The integrated model explained the highest  
28 presence/absence variance of *C. odorata* ( $D^2 = 0.57$ , i.e. 57%). This model was used to derive  
29 probability map indicating the occurrence of invasive species in forest gaps. A 2 x 2 error matrix  
30 table and the receiver operating characteristic (ROC) curves derived from an independent validation  
31 dataset ( $n = 38$ ) were used to assess the mapping accuracy. Approximately 87% of canopy gaps  
32 containing *C. odorata* were correctly predicted at probability threshold of between 0.2 and 0.3. The  
33 derived probability map of *C. odorata* occurrence will assist management in prioritizing target areas  
34 for eradication of the species.  
35

36 **Keywords:** forest management, remote sensing, invasive species, ROC curve, mapping accuracy

---

## 37 Introduction

38 Tropical forests cover approximately 6 % of the total land surface, and are important to the survival  
39 of many faunal and floral life-forms (WWF 2013). These forests also play a major role in the global  
40 climatic system, acting as carbon sinks (Sohngen and Alig 2000) and in water and nutrient cycling  
41 (Skole and Tucker 1993; Bousquet et al. 2000). Additionally, they provide ecological services to the  
42 nearby communities in the form of harvested timber, medicinal, food and wood crafts (Balee 1989;

43 Cunningham 2001). However, their sustainability is threatened by the anthropogenic activities such as  
44 settlement expansion, agriculture, industrial activities, climate change and invasive species (Fourcade  
45 1889; Geldenhuys 1989).

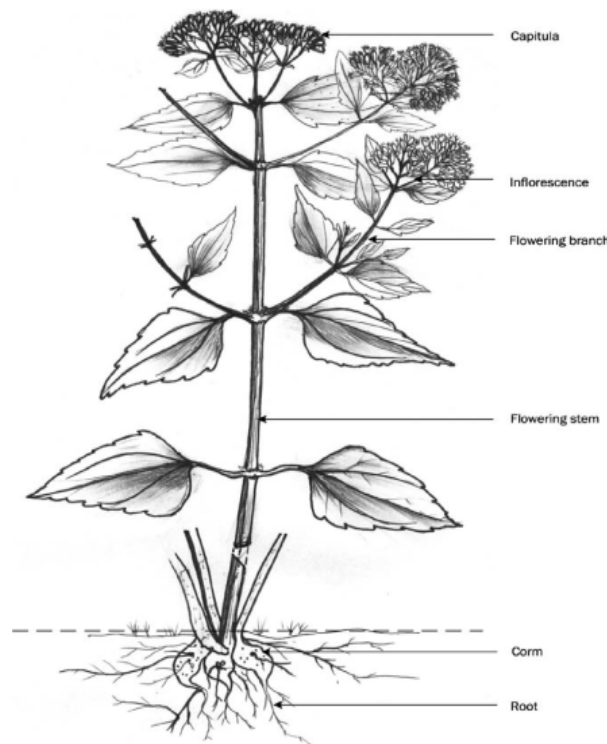
46 One of the world's most noxious alien plants is *Chromolaena odorata* (triffid weed, Fig.1.), a shrub  
47 species that is indigenous to North and Central America, and is invasive in more than 23 countries  
48 globally. The invasive *Chromolaena odorata* (here onwards referred to as *C. odorata*) has an  
49 allelopathic effect that inhibits the indigenous plant species recruitment (Goodall and Zachariades,  
50 2002; Sahid and Sugau, 1993), by changing the chemical composition of soil underneath its canopy in  
51 indigenous forests (de Rouw 1991). *C. odorata* thrives in habitats that receive sufficient sunlight,  
52 ruderal environments, close to water courses and at forest or road margins (Joshi et al. 2006). The  
53 habitat preference is facilitated by the fact that *Chromolaena* species requires sufficient light and  
54 moisture, and as such, wide open areas serve as optimal niches for its establishment and seed dispersal  
55 (Witkowski and Wilson 2001). Its tap-root system allows for deeper penetration into the substrate  
56 which gives it a competitive advantage over the native seedlings (Awanyo et al. 2011). In tropical  
57 forests, this species invades the indigenous vegetation through forest gaps, which may be created by  
58 tree fall (Kupfer and Runkle 1996), any catastrophic event (Brokaw 1982; Whitmore 1989), or  
59 selective timber harvesting (Suarez et al. 1998). The control and eradication of these invaders requires  
60 accurate mapping of forest gaps and modelling the extent of invasion in such gaps (Le Maitre et al.  
61 1996; Underwood et al. 2003). Mapping the extent of invasive species may assist forest managers,  
62 conservation practitioners and all the relevant stakeholders to comprehend the extent of invasion and  
63 to allocate limited resources for the species eradication programmes (Reyers 2004).

64 Conventionally, identification of invasive species is done using ground-based surveys (Buckland et  
65 al. 1996; Scott et al. 2002). This involves identifying species at habitats that are accessible, usually at  
66 the forest edges and in the proximity to roads and paths (Edwards et al. 2007). Although the collected  
67 environmental data (such as distance from roads and forest edges) are still useful in species prediction  
68 (Hirzel and Guisan 2002), the success of using environmental data collected through traditional field  
69 surveys is hampered by the amount of time and effort required for collection (Gu and Swihart 2004;  
70 Margules and Pressey 2000). Additionally, a major drawback of employing field surveys is that they  
71 are inefficient in larger areas and in areas with less accessible terrain (Turner et al. 2003), while it is  
72 impossible to visit all forest gaps in indigenous tropical forests. To mitigate this problem, remote  
73 sensing technology is increasingly being employed as a rapid and cost-effective alternative for  
74 mapping invasive species in their habitats (Underwood et al. 2003; Joshi et al. 2006). Remote sensing  
75 technology provides spatial vegetation cover over large geographical areas. This technology has been  
76 successfully used for actual canopy cover mapping of invasive species that dominate the canopy  
77 (Asner et al. 2008; Harding and Bate 1991). In instances where the invasive species' spectral  
78 signature does not dominate the canopy, the probabilistic mapping approach has been adopted (Joshi  
79 et al. 2006; Laba et al. 2004).

80 Few studies have been conducted to map the probability of occurrence of non-canopy dominating  
81 invasive species using remote sensing and environmental data in indigenous forests. For example  
82 Joshi et al. (2006) integrated Landsat ETM+ imagery with environmental data to map the probability  
83 of occurrence of *C. odorata* in south central Nepal forest. However, remote sensing data such as  
84 Landsat, SPOT or IKONOS consist of spectral bands whose signal tend to saturate in high canopy  
85 vegetation i.e. leaf area index (LAI) greater than three (Knipling 1970; Mutanga and Skidmore 2004).  
86 Subtropical forest gaps are usually characterised by a high LAI. The development of new generation  
87 high spatial resolution satellites such as RapidEye (5 meters) and WorldView-2 (2 meters) has opened  
88 opportunities for improved characterisation of vegetation in a high LAI environment (Ramoelo et al.

89 2012; Mutanga et al. 2012; Ozdemir and Karnieli 2011). The red edge band (700-725 nm) present in  
90 RapidEye and WorldView-2 has been shown to minimize the signal saturation problem common in  
91 traditional sensors, thereby improving the prediction of chlorophyll, nitrogen and vegetation biomass  
92 (Ramoelo et al. 2012; Mutanga et al. 2012; Cho et al. 2013). In remote sensing, the “red edge” is the  
93 region of abrupt change in the leaf reflectance between 680 and 780 nm due to the combined effect of  
94 strong chlorophyll absorption in the red and high reflectance in the near-infrared wavelength resulting  
95 from internal scattering in the spongy mesophyll (Horler et al. 1983). Could the presence of the red-  
96 edge band in WorldView-2 enhance the ability of predicting the occurrence of invasive *C. odorata* in  
97 forest canopy gaps?

98 Ancillary environmental data such as distance from roads/trails, distance from rivers, distance from  
99 forest edges that have been used to predict the distribution of species (Franklin 1995; Yang et al.  
100 2006; Václavík and Meentemeyer 2009; Masocha and Skidmore 2011) can be easily generated from  
101 remote sensing imagery. The question is: Can the integration of ancillary environmental data with  
102 WorldView-2 data increase the accuracy of predicting the probability of occurrence of invasive *C.*  
103 *odorata* in forest canopy gaps? We used Dukuduku Coastal Forest of KwaZulu-Natal province, South  
104 Africa as a case study to test the afore-mentioned assumptions. Mapping the occurrence of the  
105 invasive species in forest canopy gaps rather than its actual cover is important since *C. odorata*  
106 occupies the canopy gaps mixed with other species, as opposed to growing understorey due its light,  
107 space and soil moisture requirement (Joshi et al. 2006).



108

109 **Fig. 1** Schematic representation of *Chromolaena odorata* morphology (Source: Joshi et al. 2006)

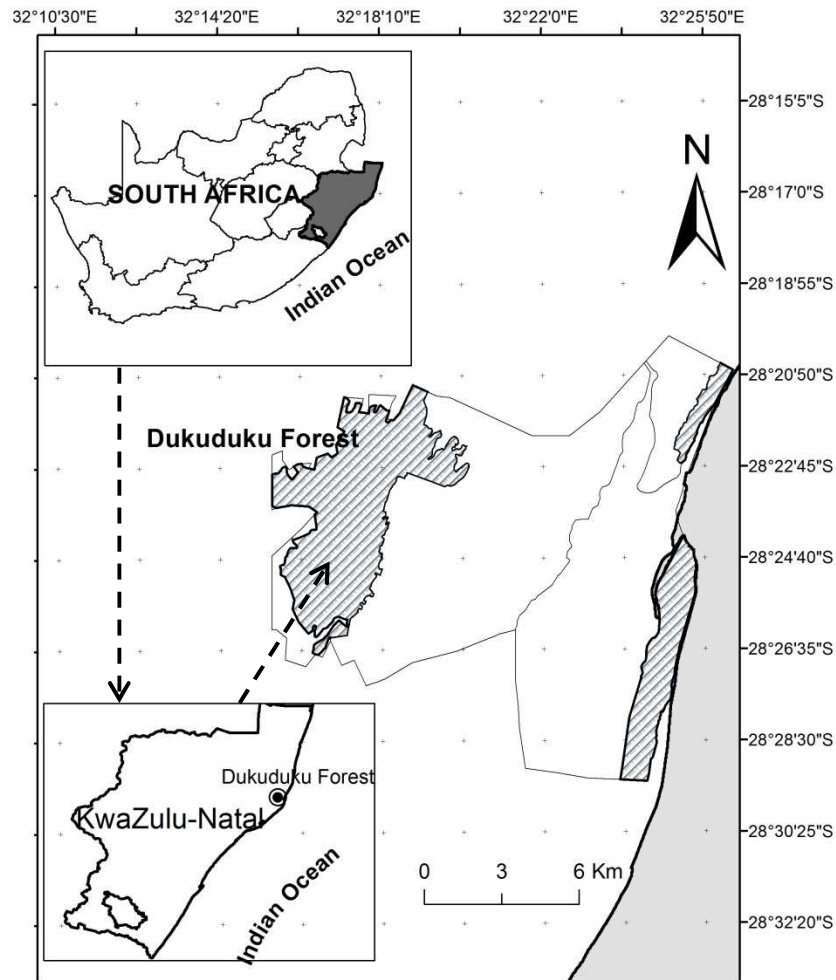
### 110 *Study area*

111

112 This study was undertaken in Dukuduku forest, the largest remaining patch of subtropical coastal  
113 forest in KwaZulu-Natal, South Africa (28°38'33"S and 32°31'67"E). (Fig. 2). The study area has an  
114 area of about 3172.43 hectares. On the western side, the forest is surrounded by the sugar plantation  
115 farms and the *Eucalyptus* plantations, while on the eastern side are villages that practise subsistence

116 farming. The climate of KwaZulu-Natal is subtropical, with high summer precipitation and high  
117 temperatures of over 33°C (between September and April). Winters are generally cooler (below 8°C),  
118 with the annual sea surface temperature of 15°C. The area receives annual rainfall of about 1 600 mm  
119 (Luwum 2002).

120



121

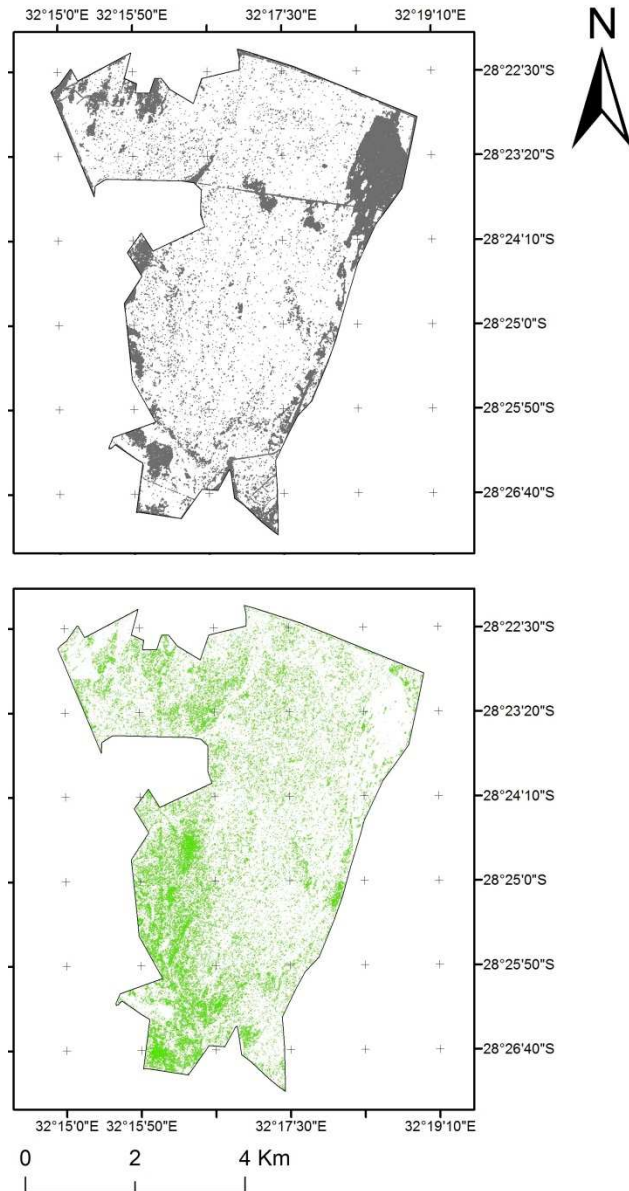
122 **Fig. 2** The location of the Dukuduku forest in KwaZulu-Natal, South Africa.

123

124 *Image acquisition and pre-processing*

125

126 WorldView-2 image (acquired on 01 December 2010) with 8 spectral bands and at a 2 meter spatial  
127 resolution was used for the delineation of forest gaps. The delineated forest gaps (**Fig. 3**) were derived  
128 from WorldView-2 data using object-based image analysis (OBIA), with a 93.69% overall accuracy  
129 (Malahlela et al. in review). The image was geo-referenced to Universal Transverse Mercator (WGS  
130 84), mosaicked and clipped to the study area. The imagery was geometrically corrected by the  
131 supplier (geolocation accuracy < 3.5m CE90, as specified by Digital Globe), and the atmospheric  
132 correction was done using the AtCOR 2/3 software distributed by ReSe® Applications. The  
133 atmospheric correction was based on the MODTRAN 5 module, which is a ‘narrow band model’  
134 atmospheric radiative transfer code – with spectral range of between 0.2 to 100 µm (Berk et al. 1998).  
135 The atmospheric conditions specified in the AtCOR software for this image processing was the  
136 ‘tropical rural’ conditions due to the nature of the study area.



138

139 **Fig. 3** Delineated forest gaps comprising of non-vegetated (upper) and vegetated (lower) gaps (Malahlela et  
 140 al. in review).

141

#### 142 *Field data collection*

143

144 Field data were collected on two occasions and in different seasons (July and October 2011) because  
 145 of logistical constraints. The data collected included the location of forest canopy gaps (using Vista  
 146 eTrex™ GPS, with maximum spatial accuracy of 4 m), as well as the presence/absence of invasive  
 147 species (*Chromolaena*) in forest gaps. The collection of the data followed a line transect method. A  
 148 total of 13 line transects were visited across the forest, each with the minimum length of about 1 km.  
 149 A simple random sampling technique was applied, where lines were randomly pre-selected to cover  
 150 most parts of the forest. In total, 115 ( $n = 115$ ) forest gaps were visited in the field. We used 2/3 ( $n =$

151 77) of the data to construct a logistic regression model while 1/3 ( $n = 38$ ) of the data was used to  
 152 validate the model.

153

154

155

156

157

158

159

160

161

162

163

164

165

166

167

168

169

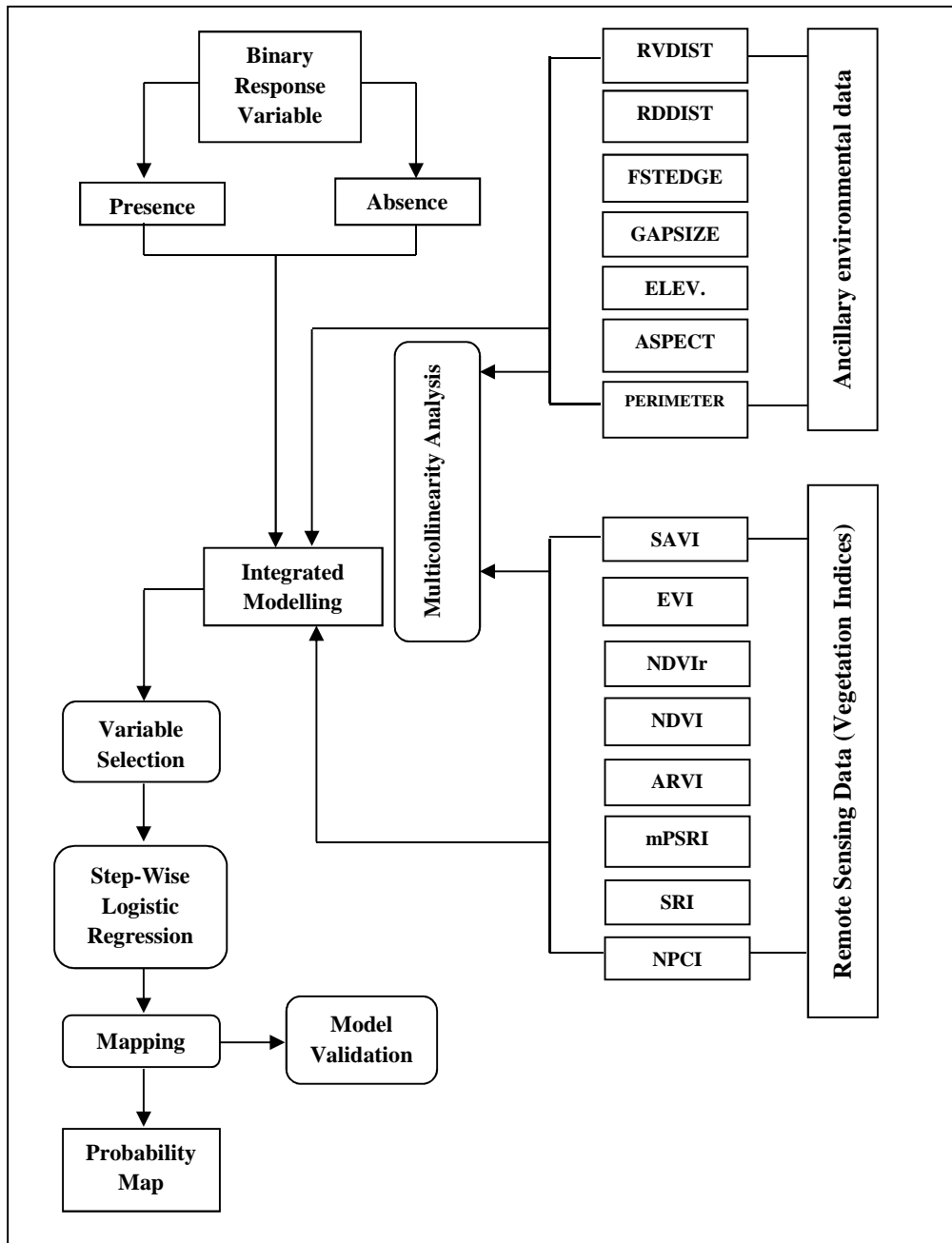
170

171

172

173

174

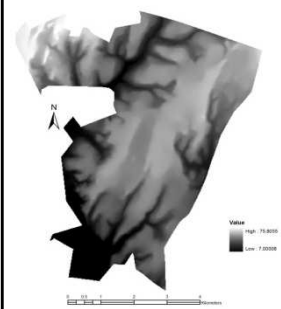
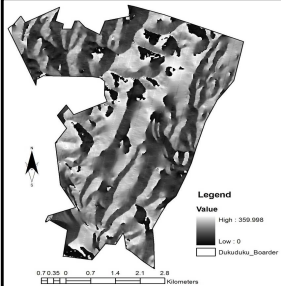
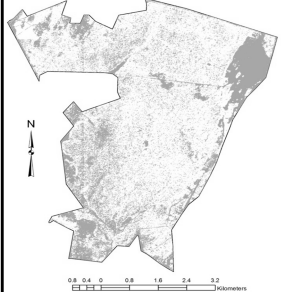
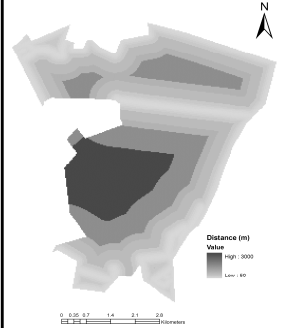


175 **Fig. 4** Schematic representation of workflow followed during logistic regression modelling.

176 *Data analysis*

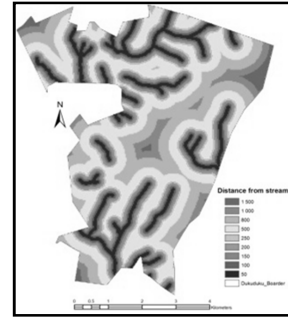
177 The relationship between *C. odorata* presence/absence, environmental data and remote sensing data  
 178 was modelled in logistic regression as shown in **Fig. 4**. A logistic regression was conducted for 3 sets  
 179 of variables, i.e. (a) environmental variables only (Table 1), (b) spectral variables only and (c)  
 180 combined environmental and remote sensing variables in a stepwise logistic regression (Table 1).

181 **Table 1**  
 182 *Ancillary environmental variables and WorldView-2 data variables used for modelling*

| Variable   | Processing  | Layer   |
|--|---|---|
| Elevation<br>(ELEV.)   | <p>The digital elevation model (DEM) layer was generated from the 15 meter contour lines of the study area</p> <p>Generation of the DEM is based on the algorithm ANUDEM, which calculates values on a regular grid of a discretised smooth surface fitted to a large number of irregularly spaced elevation data points, contour line data and stream line data (Hutchinson 1996).</p>   |    |
| Aspect<br>(ASPECT)   | <p>Aspect layer was generated from a 15 meter DEM with the help of Spatial Analyst tool in ArcGIS software</p>  |   |
| Canopy gaps characteristics (size and perimeter)<br>(GAPSIZE, PERIMETER) | <p>Gap size and gap perimeter layers were generated from the WorldView-2 derived delineated forest canopy gaps. Forest canopy gaps were delineated in object-based image analysis using the modified plant senescence index (Merzlyak et al. 1999). This technique yielded the highest accuracy of 93.69% when compared to pixel-based classification, and therefore the results were used to derive forest gap size and perimeter.</p> |  |
| Distance from roads<br>(RDDIST)  | <p>Distance from roads was generated from a road dataset in ArcGIS. The distances from roads were calculated from the forest gaps to the closest roads/paths. The forest's boundaries are mainly the main roads (national tar roads) and the gravel roads created for demarcating agricultural plantations. Distances were measured in meters (m)</p>   |  |

Distance from rivers  
(RVDIST)

The distance from river map was derived from river and streams dataset of the study area. The generation of this map was done in ArcGIS. The distance was calculated from the nearest stream to the forest gap to determine the influence of rivers to the distribution of invasive species. The distances were measured in meters (m).



Vegetation indices

Two sets of vegetation indices were tested for the regression. These sets are (i) indices that are commonly derived from conventional sensors, and (ii) indices that can be derived from WorldView-2 imagery. A total of seven (7) vegetation indices were tested for this study (Table 8).

See table 2

183

184

185 *Ancillary environmental variables*

186

Ancillary environmental variables and WorldView-2 data variables were used for modelling. Ancillary environmental data were used based on their importance as factors driving the distribution of *C. odorata* as described in the introduction and availability. The ancillary environmental dataset included digital elevation model (DEM) layer, aspect layer (ASPECT)), distance from roads layer (RDDIST), distance from rivers layer (RVDIST), gap size layer (SIZE), distance from forest edges (FSTEDGE) and gap perimeter layer (PERIMETER) (Table 1).

192

*Spectral data*

193

Spectral dataset was processed as vegetation indices. We opted to use vegetation indices as individual bands on their own do not yield any significance relationships with species occurrence (Verstraete and Pinty 1996). A number of vegetation indices such as the Normalized Difference Vegetation Index (NDVI), the Red edge Normalized Difference Vegetation Index (NDVIR), the Normalized Green Vegetation Index (NDVIGR), the Soil-Adjusted Vegetation Index (SAVI), the modified Plant Senescence Reflectance Index (mPSRI), Simple Ratio Index (SRI), the Enhanced Vegetation Index (EVI), the Normalized Pigment Chlorophyll Index (NPCl), and the Atmospherically Resistant Vegetation Index (ARVI) were computed from WorldView-2 image. These indices were treated individually as separate input variables for prediction. These indices fall into either of the two sets, i.e. (i) indices that can be commonly derived from conventional sensors such as Landsat, and (ii) indices that can be derived from WorldView-2 imagery. A total of eleven (11) vegetation indices were tested for this study (Table 1 and 2).

205

206

207

208

209

210

211

212



213  
214  
215  
216

**Table 2**  
Vegetation indices selected for the study

| Index         | Formula   | Application  | Reference                    |
|---------------|---|--|------------------------------|
| NDVI          | $NDVI = \frac{\rho_{833} - \rho_{660}}{\rho_{833} + \rho_{660}}$  | Traditional index used to monitor vegetation vigour, health, vegetation cover and biomass. Values range from -1 (bare surfaces) to 1 (green plants).   | Jackson et al.(1983)         |
| NDVIR         | $NDVIR = \frac{\rho_{833} - \rho_{725}}{\rho_{833} + \rho_{725}}$                                       | New WorldView-2 index that improves the detection of vegetation health, greenness, and biomass estimation. It is computed from the red edge band centered at 725nm, instead of a red band centered at 660nm as in NDVI. Values range from -1 (bare surfaces) to 1 (green vegetation).  | Gitelson and Merzlyak (1994) |
| SRI (various) | $SRI = \frac{\rho_{660}}{\rho_{833}}$   | Used for mapping vegetation health and condition. It is high in very healthy vegetation and low in stressed vegetation or non-vegetated areas.   | Asrar (1989)                 |
| mPSRI         | $mPSRI = \frac{\rho_{660} - \rho_{480}}{\rho_{725}}$  | New WorldView-2 index used for detecting of leaf senescence, plant physiological stress and fruit ripening. Values range from -1 (stressed canopy) to 1 (less stressed canopy).  | Merzlyak et al.(1999)        |
| NDVIGr        | $NDVIGr = \frac{\rho_{833} - \rho_{545}}{\rho_{833} + \rho_{545}}$                                      | Traditional index that works similarly to NDVI and additionally measures the greenness of vegetation.  | Gitelson et al.(1999)        |
| EVI           | $EVI = 2.5 \left( \frac{\rho_{833} - \rho_{660}}{\rho_{833} + 6\rho_{660} - 7.5\rho_{480} + 1} \right)$ | The enhanced vegetation index (EVI) is an 'optimized' index designed to enhance the vegetation signal with improved sensitivity in high biomass regions and improved vegetation monitoring through a de-coupling of the canopy background signal and a reduction in atmospheric influences.  | Huete et al.(1997)           |
| ARVI          | $ARVI = \frac{\rho_{833} - (2\rho_{660} - \rho_{480})}{\rho_{833} + (2\rho_{660} - \rho_{480})}$        | An enhancement to the NDVI that is relatively resistant to atmospheric factors (for example, aerosol). It uses the reflectance in blue to correct the red reflectance for atmospheric scattering. It is most useful in regions of high atmospheric aerosol content, including tropical regions contaminated by soot from slash-and-burn agriculture. | Kaufman and Tanre (1996)     |
| NPCI          | $NPCI = \frac{\rho_{660} - \rho_{425}}{\rho_{660} + \rho_{425}}$  | The normalized difference pigment chlorophyll index (NPCI) was developed especially for the detection of the chlorophyll content of crops.   | Peñuelas et al. (1995)       |
| SAVI          | $SAVI = \left( \frac{\rho_{830} - \rho_{660}}{\rho_{830} + \rho_{660} + 0.5} \right) * (1 + 0.5)$       | Traditional index used also for vegetation monitoring, biomass and vegetation health. It improves on NDVI by compensating for soil-background.   | Huete et al. (1997)          |

217  
218  
219

220 *Model calibration*

221 The dataset ( $n = 77$ ) was randomly split into 2/3 ( $n = 38$ ) for model calibration. The calibration  
222 dataset was used to train the model for invasive species occurrence using the R statistical software. A  
223 stepwise logistic regression model was used for all input variables. In stepwise logistic regression, an  
224 attempt is made to eliminate any insignificant variable from the model before adding a significant one  
225 to the model and to deal with multi-collinear variables. We used forward elimination procedure to  
226 select suitable variables in the final model (Manel et al. 1999). The choice of the forward stepwise  
227 logistic regression model was dictated by the binary nature of the response variable  
228 (presence/absence), its simplicity for embedding in GIS software (Yang et al. 2006) and its popularity  
229 amongst all other predictive models (Manel et al. 1999; Aspinall 2002). Logistic regression is given  
230 by the following equation:

$$231 \quad P = \frac{e^{\beta_0 + \beta_1 x_1 + \beta_2 x_2 + \dots + \beta_n x_n}}{1 + e^{\beta_0 + \beta_1 x_1 + \beta_2 x_2 + \dots + \beta_n x_n}} \quad (1)$$

232 where  $P$  is the probability of occurrence,  $x_n$  is the explanatory variable,  $\beta_n$  are the coefficient of  $x_n$ ,  $\beta_0$   
233 is the intercept and  $e$  is the exponent function of the model. The final model goodness of fit was  
234 measured by the deviance ( $D^2$ ) which is an analogy to a coefficient of determination ( $R^2$ ) peculiar to  
235 logistic regression model (Rossiter and Loza 2012). The  $D^2$  is obtained from the following equation:

$$236 \quad D^2 = 1 - \left( \frac{\text{residual deviance}}{\text{null deviance}} \right) \quad (2)$$

237  
238 Each variable removal or addition from or to a model is listed as a separate step in the model output.  
239 The model with the highest  $D^2$  and lowest Aikake's Information Criterion (AIC) was selected as the  
240 most ideal model because it has the best fit (Fox 2002).  
241

242 *Model validation*

243 One-thirds of the data ( $n = 38$ ) was used for validating the predictive model. The predicted  
244 probabilities ( $y$ ), which ranged from values between 0 and 1, represented the increasing probability of  
245 *C. odorata* presence in forest canopy gaps. A range of thresholds was explored to determine the  
246 optimum threshold level for predicting *C. odorata* presence/absence (P/A) in forest gaps. The study  
247 by Manel et al. (1999) previously suggested a probability threshold value of 0.5 as the optimum  
248 threshold value for species prediction, although this value may not be ideal in all circumstances. For  
249 this study, we tested probability thresholds of 0.2 – 0.9. A 2 x 2 error matrix table (with rows  
250 indicating predicted cases and columns indicating observed cases) was plotted for a threshold value  
251 that yielded the highest mapping accuracy. The overall mapping accuracy is defined as the total  
252 number of the correctly predicted test cases to the total number of test samples, and is presented as a  
253 percentage (Fielding and Bell 1997). The table compares the predicted values (from an optimum  
254 threshold value) with the observed field data of *C. odorata* distribution.

255 The area under the ROC (AUC) has been used in several studies in order to understand the  
256 robustness of the model for a binary classifier (Egan 1975; Swets et al. 2000; Fawcett 2006; MedCal  
257 2014). The AUC value of 0.5 indicates that the model accuracy is equal to the random prediction,  
258 while the value of 1.0 shows the perfect model fit (Baldwin 2009). In essence, the AUC has a  
259 quantitative measure on a 0.0 to 1.0 scale, with the following grading levels:

- 260
- < 0.6 indicates a poor model

- 261 • 0.6 – 0.7 indicates a pass model
- 262 • 0.7 – 0.8 indicates a good model
- 263 • >0.9 indicates an excellent model

264 Furthermore, the sensitivity and specificity analysis was performed across the probability range  
 265 from 0.2 – 0.9. For binary error matrix, sensitivity is defined as the proportion of correctly classified  
 266 presence to the total number of presences in the test samples. On the other hand, specificity is the  
 267 proportion of correctly predicted absence to the total number of absence in test samples (Fielding and  
 268 Bell 1997).

## 269 Results

### 270 Logistic regression

271 The combined environmental and spectral data model explained 71 % of the variance in the *C.*  
 272 *odorata* presence/absence data ( $D^2 = 0.71, p < 0.05$ ), which was the highest when compared to the  
 273 spectra data only ( $D^2 = 0.30, p < 0.05$ ) and ancillary environmental data only ( $D^2 = 0.52, p < 0.05$ )  
 274 models. From the integrated stepwise logistic model, two of the environmental variables (distance  
 275 from rivers and distance from roads) were significant at  $p < 0.05$ . These environmental variables have  
 276 shown negative relationship to the presence/absence of *C. odorata* in the forest gaps, at  $p < 0.05$ .

277  
 278 **Table 3**

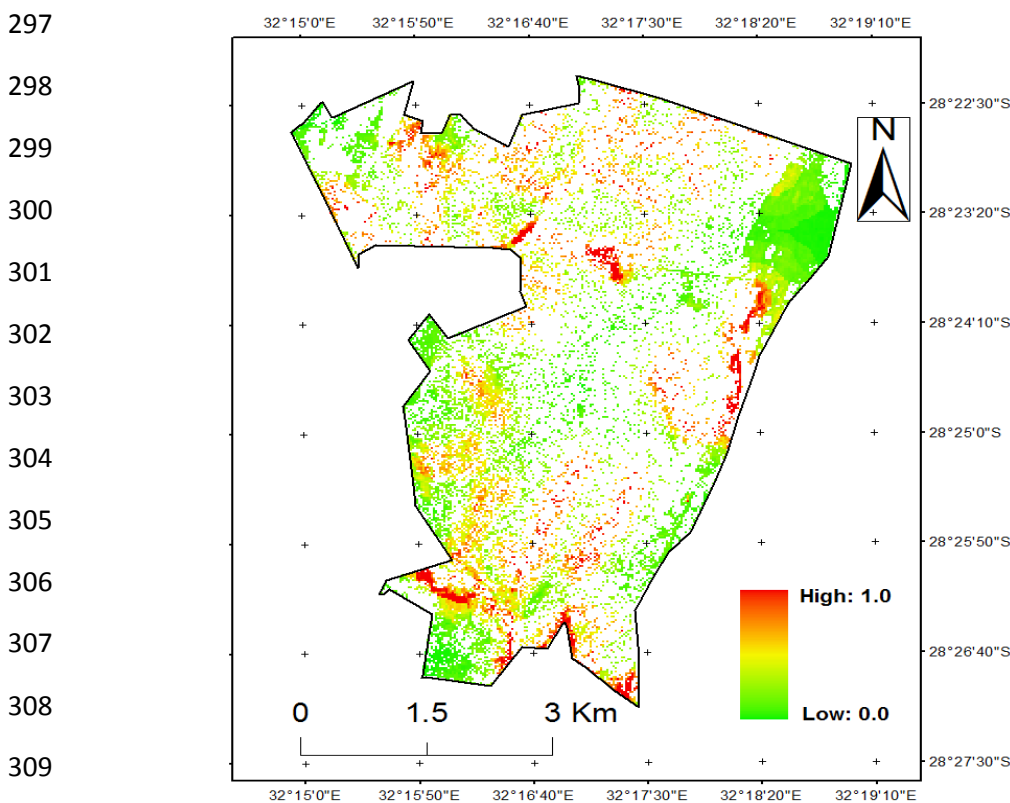
279 The results of three logistic regression models and their significant (shown by \* and °) and non-significant  
 280 variables.  
 281

| Data Source                                 | Predictor            | Estimate   | Std. Error | z value | $\rho$ value |
|---|----------------------|------------|------------|---------|--------------|
| Environmental Variables<br>( $D^2 = 0.52$ ) | (Intercept)          | 5.9560     | 2.2394     | 2.2660  | 0.007 **     |
|   | Distance from rivers | - 0.0059   | 0.0023     | - 2.601 | 0.009 **     |
|   | Distance from roads  | - 0.0033   | 0.0014     | - 2.400 | 0.016 *      |
|   | Elevation            | - 0.0230   | 0.0334     | - 0.689 | 0.490        |
|   | Aspect               | 0.0029     | 0.0051     | 0.582   | 0.561        |
|   | Gap Size             | 0.0275     | 0.0200     | 1.372   | 0.169        |
|   | Distance from edges  | - 0.0013   | 0.0013     | - 0.982 | 0.326        |
|   | Gap perimeter        | - 0.0509   | 0.0363     | - 1.401 | 0.161        |
| WorldView-2 Variables<br>( $D^2 = 0.30$ )   | (Intercept)          | - 273.080  | 273.274    | - 0.999 | 0.317        |
|   | NDVIgr               | 14.506     | 14.632     | 0.991   | 0.322        |
|   | SRI_r                | 803.929    | 380.604    | 2.112   | 0.035 *      |
|   | SRI_IR               | - 1.900    | 1.021      | - 1.861 | 0.063 °      |
|   | SRI_re               | - 281.530  | 143.338    | - 1.964 | 0.050 *      |
|   | NDVIr                | - 361.554  | 190.469    | - 1.898 | 0.058 °      |
|   | mPSRI                | - 347.555  | 163.974    | - 2.120 | 0.034 *      |
|   | SAVI                 | 1861.780   | 1066.201   | 1.746   | 0.081 °      |
|   | NDVI                 | - 1907.697 | 1460.870   | - 1.306 | 0.192        |
|   | ARVI                 | - 322.005  | 192.147    | - 1.676 | 0.093 °      |
|   | NPCI                 | 10.572     | 21.089     | 0.501   | 0.616        |
| EVI   | - 0.986              | 4.297      | - 0.229    | 0.819   |              |
| Combined Model<br>( $D^2 = 0.57$ )          | (Intercept)          | 114.600    | 62.26      | 1.840   | 0.066 °      |
|   | Distance from rivers | - 0.0200   | 0.0100     | - 2.121 | 0.033 *      |
|   | Distance from roads  | - 0.0100   | 0.0000     | - 2.225 | 0.026 *      |
|   | NDVIr                | - 38.110   | 24.770     | - 1.538 | 0.123        |
|   | SAVI                 | - 76.920   | 42.190     | - 1.823 | 0.068 °      |
|   | mPSRI                | - 291.80   | 167.70     | - 1.740 | 0.081 °      |

|  |          |        |         |         |
|--|----------|--------|---------|---------|
| NDVIgr   | 68.910   | 51.750 | 1.823   | 0.183   |
| EVI  | - 19.000 | 10.780 | - 1.763 | 0.078 ° |
| Elevation  | - 0.0900 | 0.0500 | - 1.922 | 0.050 ° |
| <i>Significance codes:</i> (°), 0.1 (°), 0.1 (*) , 0.05 (**), 0.01 (***) , 0.001 |          |        |         |         |

282 The elevation was the only environmental variable with a significant negative relationship to the  
 283 presence/absence of invasive species ( $p < 0.05$ ). Additionally, from this model, three of the spectral  
 284 data variables (mPSRI, SAVI and EVI) were significant at  $\alpha < 0.1$ . All of the vegetation indices  
 285 have shown negative correlation to the invasive *C. odorata* presence/absence in forest gaps. On the  
 286 other hand, the NDVIgr showed a positive relationship to the presence/absence data of *C. odorata* in  
 287 forest gaps (Table 3). The results from environmental data-only model have shown that the intercept  
 288 ( $p < 0.01$ ), distance from roads ( $p < 0.01$ ), and distance from roads/paths ( $p < 0.05$ ) were significantly  
 289 correlated to species presence/absence. Among the environmental data only model, the distance from  
 290 rivers was the most significant positive variable at  $p < 0.01$ . Amongst WorldView-2 data only  
 291 model, six of the variables were significant, with red Simple Ratio Index (SRI\_r, computed from  
 292 red/NIR1), the red edge Simple Ratio Index (SRI\_re, computed from red edge/NIR1) and mPSRI  
 293 were significantly correlated to the species presence/absence in the forest gaps at  $p < 0.05$ . Figure 5  
 294 shows the predicted probability of occurrence of invasive species across the delineated forest gaps.

295 Overall, the integrated step-wise logistic regression model has shown an improvement of over 36%  
 296 compared to environmental variables only.



310 **Fig. 5** A predicted probability map indicating the occurrence of *Chromolaena odorata* in delineated forest  
 311 gaps at the Dukuduku forest.

### 312 *Model validation*

313 The predictive model (binary outcome value range of 0.0 – 1.0) was validated using probability  
 314 threshold values as shown in table 4. The highest prediction accuracies were obtained at threshold

315 range between 0.2 and 0.3 (both at 87%). The highest sensitivity rates (defined as the proportion of  
 316 correctly classified presence to the total number of presences in the test samples) were observed at  
 317 similar threshold range (87%). The highest specificity rates (specificity is the proportion of correctly  
 318 predicted absence to the total number of absence in test samples) were obtained at the threshold  
 319 values of 0.8 and 0.9 (both at 86%) (Fielding and Bell 1997). The 2 x 2 error matrix table for a  
 320 probability threshold of 0.2 and 0.3 is shown in table 5.

321

322 **Table 4**  
 323 Statistics for evaluating model performance across probability threshold values

|                         | Probability Threshold |      |      |      |      |      |      |      |
|-------------------------|-----------------------|------|------|------|------|------|------|------|
|                         | 0.2                   | 0.3  | 0.4  | 0.5  | 0.6  | 0.7  | 0.8  | 0.9  |
| Prediction Accuracy (%) | 0.87                  | 0.87 | 0.84 | 0.84 | 0.84 | 0.82 | 0.82 | 0.79 |
| Sensitivity (%)         | 0.87                  | 0.87 | 0.84 | 0.84 | 0.84 | 0.81 | 0.81 | 0.77 |
| Specificity (%)         | 0.86                  | 0.86 | 0.86 | 0.86 | 0.86 | 0.86 | 0.86 | 0.86 |

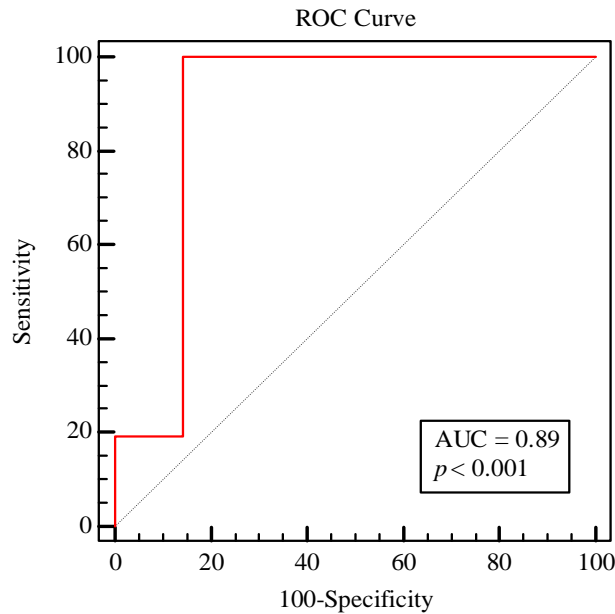
324

325 **Table 5**  
 326 Predicted outcomes (y) from logistic regression on *Chromolaena odorata* vs. the observed field data at  
 327 probability threshold of 0.2 and 0.3 ( $\rho = 0.3$ )  
 328

|                      |          | Predicted Occurrences |         |       |
|----------------------|----------|-----------------------|---------|-------|
|                      |          | Presence              | Absence | Total |
| Observed Occurrences | Presence | 27                    | 4       | 31    |
|                      | Absence  | 1                     | 6       | 7     |
|                      | Total    | 28                    | 10      | 38    |

329

330 The robustness of the model (curve) was also measured by the Area Under the Curve of receiver  
 331 operating characteristic (ROC) curve (Fig. 6). The validation dataset yielded an AUC of 0.89 at  $p =$   
 332 0.001, which shows that the model used for prediction was significant. The diagonal line in the model  
 333 represents the strategy of randomly guessing a class (Fawcett 2006). If the curve bends towards or  
 334 below the diagonal line (decreasing sensitivity) this indicates a poor model. A good model is the one  
 335 whose curve bends towards the north-western direction of the plot (Fawcett 2006). Our ROC shows  
 336 that our curve bends towards the north-western direction, and hence an AUC of 0.89.



337

338 **Fig. 6** The ROC curve derived from validation dataset ( $n = 38$ ) across different probability thresholds. The  
 339 dotted line indicates a line of no-discrimination (random guess) while the red line indicates sensitivity and  
 340 specificity of model across different threshold values.

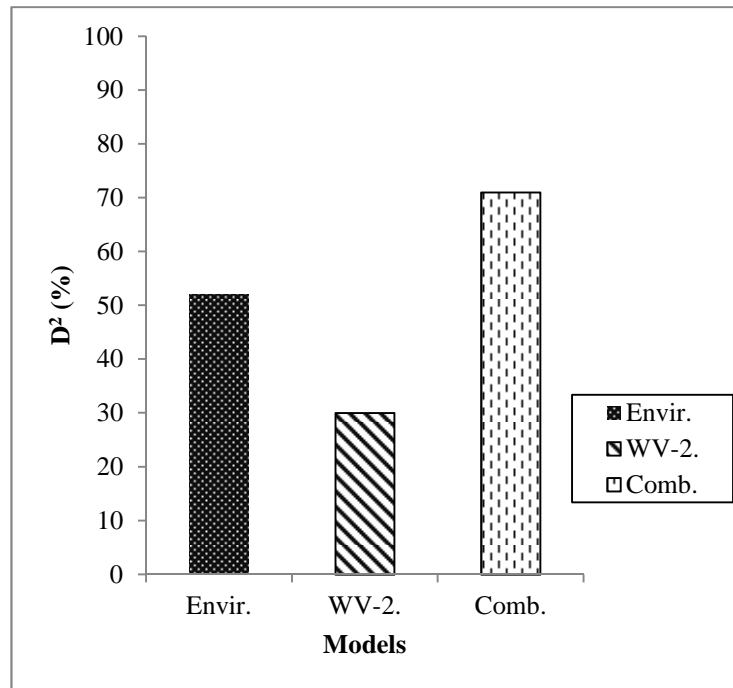
341

## 342 Discussion

343 The findings of the study suggest that there is a relationship between WorldView-2 spectral bands  
 344 and the presence/absence of invasive *C. odorata* (Table 3). The model that combined the  
 345 environmental variables and spectral variables yielded the highest prediction accuracy, which  
 346 underscores the importance of such variables in the prediction of *C. odorata* in forest gaps (Ozdemir  
 347 and Karnieli 2011) (Fig. 7). This integration is necessary since on their own, the ancillary  
 348 environmental variables or WorldView-2 data do not yield prediction accuracies greater than 60%.  
 349 The general trend depicted by the predictive model shows that the probability of occurrence of *C.*  
 350 *odorata* tends to increase in forest gaps that are less vegetated than those that are densely vegetated.  
 351 This trend is supported by observing the predictive model's spectral estimates of the NDVIr, mPSRI,  
 352 SAVI and EVI, most of which are significantly correlated with the presence and absence data of *C.*  
 353 *odorata*. A negative estimate of red edge band (used to compute NDVIr) means that the presence of  
 354 *C. odorata* decreases with increasing density of vegetation, as an increase in reflectance at this  
 355 spectral region (705 – 745 nm) is associated with increases in vegetation densities or biomass  
 356 (Knipling 1970). Similar findings were achieved by Joshi et al. (2006) who observed that *C. odorata*  
 357 does not thrive in densely vegetated forest areas. This characteristic is very important to this invader,  
 358 in that it satisfies the light requirement of the species in question. These findings show that the red  
 359 edge is significant in mapping the probability of occurrence of *C. odorata*.

360 Previous studies have highlighted that the plant senescence reflectance index (PSRI, from which  
 361 mPSRI was derived) is sensitive for detecting senescing leaves and to detect physiological stress at  
 362 different developmental stages of plants (Merzlyak et al 1999; Peñuelas et al 1994; Hatfield and  
 363 Prueger 2010). In the same light the mPSRI (which uses blue and red edge band, instead of green and  
 364 NIR) indicated that increase in plant stress in vegetated forest gaps increases the probability of *C.*  
 365 *odorata* presence. This is true when observing the negative estimate of mPSRI (-291.80,  $p < 0.08$ )

366 since a negative estimate indicates the stressed vegetated area, while the positive estimate indicates  
 367 less stressed vegetated areas (Merzlyak et al 1999). The enhanced vegetation index (EVI) has long  
 368 been used to assess vegetation biomass in different biomes, and it is already established that increase  
 369 in EVI values is associated with increase in the density of vegetation (Huete et al 1997). Conversely,  
 370 our study has found that decreases in EVI values is associated with the probability of invasive species  
 371 presence in forest gaps, which is an indication that less vegetated forest gaps are prone to invasion  
 372 than their vegetated counterparts. These findings are especially true considering the negative  
 373 correlation between invasive species distribution and SAVI, which is known to improve on NDVI by  
 374 compensating for soil background (Huete et al. 1997).



375  
 376 Fig. 7 Model accuracy comparison amongst environmental data-only model (Envir), WorldView-2 data-only  
 377 (WV-2) and a combined environmental and WorldView-2 data model (Comb).

378 The environmental variables such as distance from rivers/streams and aspect were found to be  
 379 negatively significant in determining the presence and absence of *C. odorata* occurrence. The  
 380 implication is that as one advances closer to the streams, the probability of finding *C. odorata*  
 381 increases, and this is in line with the findings by Joshi et al. (2006) and Van Gils et al. (2006) who  
 382 found areas closer to roads and edges to be more likely invaded by *C. odorata*. The tap root system of  
 383 this species gives it a competitive advantage over water and ensures its stability in invaded habitats.  
 384 The results also showed that the probability of invasive species occurrence increases with the decrease  
 385 in elevation. This is true since in troposphere an increase in elevation results in decrease in  
 386 temperature, and thereby inhibiting the occurrence of plant species that are adapted to warmer  
 387 conditions. Additionally, one is more likely to find invasive species in north facing slopes, than the  
 388 south facing slopes, as shown in Table 3. This is due to the fact that north-facing slopes in the  
 389 southern hemisphere are warmer than south-facing slopes (Adams 2010). The species triumphs in  
 390 areas that are open, with appropriate light and temperature ranges of between 20 - 37°C, and hence the  
 391 increase in slope direction (towards the north) increases probability of finding *C. odorata* (Gareeb  
 392 2007). Our study also highlighted that invasive *C. odorata* prefers forest gaps that are closer to the  
 393 streams due to their competitive nature for water and essential mineral resources. This trend is in line  
 394 with the findings by Goodall and Zacharias (2002) who observed that this invasive species prefers

395 forest margins and is often found along rivers or streams. Roads and forest edges serve as the  
396 alleys/corridors through which the seeds of this species are dispersed, especially considering the fact  
397 that they require wind as a dispersal mechanism. On the whole, the pattern of the probability of  
398 occurrence (fig. 5) indicate that *C. odorata* is less likely to occur in pristine forest than in the areas  
399 that are open, such as closer to the roads or at the edges of forest (Joshi et al. 2006).

400

#### 401 *Management of invasive species*

402 The management of invasive species such as *C. odorata* has been debated in different countries,  
403 globally. For example Herren-Gemill (1991) described the need to control *C. odorata* due to its high  
404 frequency of occurrence in invaded fallow sites in West Africa. From the conservation point of view,  
405 management and control priority should be focused on the species' habitat and future distribution of  
406 species (Rowe 1992), and not solely on the degradation levels caused by this species (Goodall and  
407 Erasmus 1996). Mapping the probability of occurrence of invasive species in its potential habitats  
408 (forest gaps) is crucial to the management geared towards eliminating such species. The output maps  
409 serve as a guideline to fieldworkers and forest managers for the identification of probable habitats of  
410 *C. odorata* and for man-power recruitment.



411

412 **Fig. 8** Probability maps are crucial to the management of invasive species. In these picture frames the  
413 researcher (Primary author of this paper) presents the probability maps to the field workers who were  
414 tasked to eradicate invasive *Chromolaena odorata* in across the forest.

415 In South Africa, for example, there are projects that are aimed at eradicating invasive *C. odorata* in  
416 the coastal forests, such as the Dukuduku forest (Fig.8), where field workers are assigned to walk  
417 randomly through the forest to eradicate visible invasive species. The modeling of invasive species  
418 probability of occurrence could potentially assist in eliminating the random search of invasive species  
419 by providing key indications of areas of high probability of occurrence. Additional environmental  
420 data variables such as mean annual temperature, precipitation, soil data (pH, texture, moisture), could  
421 potentially improve the prediction power of the model. The application of predictive models such as  
422 Maxent has also shown to increase the prediction accuracy of species presence/absence data but has  
423 not been used for the study (Kumar and Stohlgren, 2009).

424



### 425 3.6 Conclusion

426 The additional bands present in WorldView-2 bands increases the capability of the sensor in the  
427 mapping of the probability *C. odorata* presence/absence in subtropical forest canopy gaps when  
428 compared to ancillary environmental variables. The improved accuracies are derivable when using  
429 WorldView-2 data products such as vegetation indices. The environmental data-only model explained  
430 about 52% of the presence/absence of invasive *C.odorata* presence or absence in forest gaps. The  
431 final combined model of WorldView-2 spectral data and ancillary environmental data increased  
432 predictive model accuracy to 71% ( $D^2 = 0.71$ ; WorldView-2 data added) from 52 % ( $D^2 = 0.52$ ;  
433 environmental data only), which emphasizes the advantage of integrating WorldView-2 with the  
434 ancillary environmental data for invasive species mapping. From the selected model, all other  
435 vegetation indices have shown the expected pattern of the distribution of *C. odorata* in forest gaps,  
436 except the green normalized difference vegetation index (NDVIgr), which has shown to be  
437 insignificantly positively related to invasive species in forest gaps. Although this variable contributed  
438 to the model, its implication to invasive species occurrence is subject to further investigation.  
439 Exploring the indices centered on new bands of WV-2 such as coastal band, yellow band and near-  
440 infrared-2 could potentially increase the accuracy of prediction, rather than red edge-centric analysis.

441

### 442 Acknowledgments

443 We wish to thank the Council for Scientific and Industrial Research's Natural Resources and  
444 Environment (CSIR-NRE) unit, of South Africa, for its financial assistance through its research  
445 grants. Many thanks also to the Department of Agriculture, Forestry and Fisheries for the support on  
446 the study area. Authors like to thank the Department of Science and Technology of South Africa for  
447 their financial support. Many thanks to Dr. R Mathieu for his leadership role at Earth Observation  
448 Group of NRE and Dr. Ramoelo for assisting with field work and insights on this paper. We  
449 appreciate the statistics tutorship assistance offered by Dr. Pravesh Debba and Nontembeko Dudeni-  
450 Tlhone of CSIR's Built Environment (CSIR-BE). Authors wish to thank Sibuyiselo Gumede of Khula  
451 village who assisted in field data collection. To Tino, my dearest son.

452

### 453 References

454

- 455 Adams J (2010) Vegetation – Climate Interaction. “How Plants Make the Global Environment”.  
456 Second Edition, Springer. ISBN 978-3-642-00880-1.
- 457 Adams J (2010) Vegetation – Climate Interaction. “How Plants Make the Global Environment”.  
458 Second Edition, Springer. ISBN 978-3-642-00880-1.
- 459 Asner GP, Knapp DE, Kennedy-Bowdoin T, Jones MO, Martin RE, Boardman J, Hughes RF (2008)  
460 Invasive species detection in Hawaiian rainforests using airborne imaging spectroscopy and  
461 LiDAR. *Rem Sens of Envir* 112: 1942-1955.
- 462 Aspinall R (2002) The use of logistic regression for validation of maps of the spatial distribution of  
463 vegetation species derived from high spatial resolution hyperspectral remotely sensed data. *Ecol*  
464 *Model* 157: 301-312.

- 465 Asrar G (1989) Theory and applications of optical remote sensing. John Wiley & Sons, Inc. New  
466 York – Chichester – Brisbane – Toronto – Singapore: 734.
- 467 Awanyo L, Attuah EM, McCarron M (2011) Rehabilitation of forest-savannas in Ghana: the impacts  
468 of land use, shade, and invasive species on tree recruitment. *Appl Geogr* 31: 181-190.
- 469 Baldwin RA (2009) Use of Maximum Entropy Modelling in Wildlife Research. *Entr* 11: 854-866.
- 470 Balée W (1989) The culture of Amazonian forests. In. D.A.Posey and W. Balée, eds., *Resource*  
471 *Management in Amazonia: Indigenous and Folk Strategies*. *Adv in Econ Bot* 7: 1-21. Bronx: New  
472 York Botanical Garden.
- 473 Berk A, Bernstein L, Anderson G, Acharya P, Robertson D, Chetwynd J, Adler-Golden S (1998)  
474 MODTRAN cloud and multiple scattering upgrade with application to AVIRIS. *Rem Sens of*  
475 *Envir* 65: 367-375.
- 476 Bousquet P, Peylin P, Ciais P, Le Quéré C, Friedlingstein P, Tans PP (2000) Regional Changes in  
477 Carbon Dioxide Fluxes of land and Oceans Since 1980. *Sci* 290: 1342-1346.
- 478 Brokaw NVL (1982) The definition of Treefall gap and its effect on measures of forest dynamics.  
479 *Biotrop* 14: 158-160.
- 480 Buckland ST, Elston DA, Beaney SJ (1996) Predicting distributional change, with application to bird  
481 distributions in northeast Scotland. *Glob Ecol and Biogeo Lett* 5: 66-84.
- 482 Chen Q (2009) Improvement of the Edge-based Morphological (EM) method for lidar data filtering.  
483 *Int J of Rem Sens* 30: 1069-1074.
- 484 Cho MA, Ramoelo A, Debba P, Mutanga O, Mathieu R, Van Deventer H, Ndlovu N (2013) Assessing  
485 the effects of subtropical forest fragmentation on leaf nitrogen distribution using remote sensing  
486 data. *Landsc Ecol* 28: 1479-1491.
- 487 Cunningham AB (2001) *Applied ethnobotany: people, wild plant use and conservation*. Earthscan,  
488 London.
- 489 de Rouw A (1991) The invasion of *Chromolaena odorata* (L.) King and Robinson (ex *Eupatorium*  
490 *odoratum*), and competition with the native flora, in a rain forest zone, south-west Cote d'Ivoire. *J*  
491 *of Biogeo* 18: 13 – 23.
- 492 Edwards TC, Cutler DR, Beard KH, Gibson J (2007) Predicting invasive plant species occurrences in  
493 national parks: a process for prioritizing prevention. Final Project Report No. 2007-1, USGS Utah  
494 Cooperative Fish and Wildlife Research Unit, Utah State University, Logan, UT 84322-5290 USA.
- 495 Egan JP (1975) *Signal detection theory and ROC analysis*, Series in Cognition and Perception.  
496 Academic Press, New York.
- 497 Fawcett T (2006) An introduction to ROC analysis. *Patt Recog Lett* 27: 861-874.
- 498 Fielding AH, Bell JF (1997) Review methods for the assessment of prediction errors in conservation  
499 presence/absence models. *Envir Conserv* 24: 38-49.
- 500 Fourcade, H.G., 1889, Report on the Natal forests, 197 pp. W. Watson, Pietermaritzburg.

- 501 Fox J (2002) Linear mixed models - An R and S-PLUS Companion to Applied Regression. R  
502 Development Core Foundation.
- 503 Franklin J (1995) Predictive vegetation mapping: geographic modeling of biospatial patterns in  
504 relation to environmental gradients. *Prog in Phys Geog* 19: 474-499.
- 505 Gareeb M (2007) Investigating in the potted *Chromolaena odorata* (L.) R.M. King and H. Robinson  
506 (*Asteraceae*). Thesis: School of Biological and Conservation Sciences, University of KwaZulu-  
507 Natal, Durban South Africa, 3-48.
- 508 Geldenhuys, C. J., 1989, Biogeography of the mixed evergreen forests of southern Africa. Ecosystems  
509 Programmes Occasional Report no. 45. FRD, Pretoria.
- 510 Gitelson A, Merzlyak MN (1994) Spectral reflectance changes associated with autumn senescence of  
511 *Aesculus hippocastanum* L. and *Acer platanoides* L. leaves. Spectral features and relation to  
512 chlorophyll estimation. *J Plant Physiol* 143:286-292.
- 513 Gitelson AA, Stark R, Kaufman YZ, Rundquist D (1999) A Technique for remote estimation of  
514 percent vegetation fraction, In Proc. the International Symposium on Spectral Sensing Research,  
515 Systems and Sensors for the New Millennium, *Int. Soc for Photogry and Rem Sens*, Oct. 31-Nov.  
516 4, 1999, Las Vegas NV,191-201.
- 517 Goodall JM, Erasmus DJ (1996) Review of the status and integrated control of the invasive weed,  
518 *Chromolaena odorata*, in South Africa. *Agric, Ecos and Envir* 56: 151-164.
- 519 Goodall JM, Zacharias P (2002) Managing *Chromolaena odorata* in subtropical grasslands in  
520 KwaZulu-Natal, South Africa. In: Zachariades, C., Muniappan, R., Strathie, L (eds). *Proceedings*  
521 *of the 5<sup>th</sup> international workshop on biological control and management of Chromolaena odorata*.  
522 ARC-PPRI, Pretoria, South Africa: 120-127.
- 523 Gu W, Swihart RK (2004) Absent or undetected? Effects of non-detection of species occurrence on  
524 wildlife – habitat models. *Biol Conserv* 116: 195-203.
- 525 Harding GB, Bate GC (1991) The occurrence of invasive *Prosopis* species in the northe-western  
526 Cape, South Africa. *S Afr J of Sci* 87: 188-192.
- 527 Hatfield JL, Prueger JH (2010) Value of using different vegetative indices to quantify agricultural  
528 crop characteristics at different growth stages under varying management practices. *Rem Sens* 2:  
529 562-578.
- 530 Herren-Gemmill B (1991) The ecological role of the exotic *Asteraceous Chromolaena odorata* in the  
531 bush fallow farming system of West Africa. *Biotrop. Special Publication* 44: 11-22.
- 532 Hirzel AH, Guisan A (2002) Which is the optimal sampling strategy for habitat suitability modelling?  
533 *Ecol Mod* 157: 33-41.
- 534 Horler DNH, Dockray M, Barber J (1983) The red edge of plant leaf reflectance. *Int J of Rem Sens* 4:  
535 273-288.
- 536 Huete AR, Liu HG, Batchily K, Leeuwen, WJ (1997) A Comparison of Vegetation Indices over a  
537 Global Set of TM Images for EOS-MODIS. *Rem Sens of Envir* 59:440-451.

538 Hutchinson M F (1996) A locally adaptive approach to the interpolation of digital elevation models.  
539 In Proceedings, Third International Conference/Workshop on Integrating GIS and Environmental  
540 Modeling, Santa Fe, NM, January 21-26, 1996. Santa Barbara, CA: National Center for  
541 Geographic Information and Analysis.

542 Jackson RD, Pinter Jr PJ, Reginato RJ (1983) Discrimination of growth and water stress in wheat by  
543 various vegetation indices through clear and turbid atmospheres. *Rem Sens of Envir* 13: 187-208.

544 Joshi C, de Leeuw J, Skidmore AK, van Andel J, Lekhak HD, van Duren IC (2006) Indirect remote  
545 sensing of a cryptic forest understorey invasive species. *For Ecol Mngt* 225: 245–256.

546 Kaufman YJ, Tanré D (1996) Direct and Indirect Methods for Correcting the Aerosol Effect on  
547 Remote Sensing. *Rem Sens of Envir* 55: 65-79.

548 Knipling EB (1970) Physical and physiological basis for the reflectance of visible and near-infrared  
549 radiation from vegetation. *Rem Sens of Envir* 1: 155-159.

550 Kumar S, Stohlgren TJ (2009) Maxent modeling for predicting suitable habitat for threatened and  
551 endangered tree *Canacomyrica monticola* in New Caledonia. *J of Ecol and Nat Envir* 1: 95-98.

552 Kupfer, JA, Runkle JR (1996) Early gap successional pathways in a *Fagus-Acer* forest preserve:  
553 patterns and determinants. *J. Veg. Sci.* 7: 247-256.

554 Laba M, Smith S, Richmond ME (2004) Purple loosestrife research and mapping for the Hudson  
555 River Valley study area. Final Report, New York Cooperative Fish and Wildlife Research Unit,  
556 Department of Natural Resources, Cornell University, Ithaca, NY.

557 Le Maitre DC (2002) Invasive alien trees and water resources in South Africa: case studies of the  
558 costs and benefits of management. *For Ecol Mngt* 160: 143-159.

559 Luwum P (2002) Control of Invasive *Chromolaena odorata*: An evaluation in some land use types in  
560 KwaZulu Natal, South Africa.

561 Malahlela, OE, Cho MA, Mutanga O (in review) Mapping canopy gaps in an indigenous subtropical  
562 coastal forest using high resolution WorldView-2 data. *Int J of Rem Sensing*.

563 Manel S, Dias JM, Ormerod SJ (1999) Comparing discriminant analysis, neural networks and logistic  
564 regression for predicting species' distributions: a case study with a Himalayan river bird. *Ecol*  
565 *Model* 120: 337-347.

566 Margules CR, Pressey RL (2000) Systematic Conservation Planning. *Nat* 405: 243-253.

567 Masocha M, Skidmore AK (2011) Integrating common classifiers with a GIS expert system to  
568 increase the accuracy of invasive species mapping. *Int J Appl Earth and Observ Geoinf* 13: 487-  
569 494.

570 MedCal (2014) Statistics for biomedical research software. Version 13.0.

571 Merzlyak JR, Gitelson AA, Chivkunova OB, Rakitin VY (1999) Non-destructive Optical Detection of  
572 Pigment Changes During Leaf Senescence and Fruit Ripening. *Phys Plant* 106: 135-141.

573 Mutanga O, Adam E, Cho MA (2012) High density biomass estimation for wetland vegetation using  
574 WorldView-2 imagery and random forest regression algorithm. Int J of Appl Earth Observ and  
575 Geoinf 18: 399-406.

576 Mutanga O, Skidmore AK (2004) Narrow band vegetation indices solve the saturation problem in  
577 biomass estimation. Int J of Rem Sens 25: 3999-4014.

578 Ozdemir I, Karnieli A (2011) Predicting forest structural parameters using the image texture derived  
579 from WorldView-2 multispectral imagery in a dryland forest, Israel. Int J of Appl Earth Observ  
580 and Geoinf 13: 701-710.

581 Peñuelas J, Baret F, Filella I (1995) Semi-empirical indices to assess carotenoids/chlorophyll a ratio  
582 from leaf spectral reflectance. Photosyn 31: 221-230.  
583

584 Peñuelas J, Gamon JA, Fredeen AL, Merino J, Field CB (1994) Reflectance indices associated with  
585 physiological changes in nitrogen- and water-limited sunflower leaves. Rem Sens of Envir 48: 135  
586 - 146.  
587

588 Ramoelo A, Skidmore AK, Cho MA, Schlerf M, Mathieu R, Heitkonig IMA (2012) Regional  
589 estimation of savanna grass nitrogen using the red-edge band of the spaceborne RapidEye sensor.  
590 Int J of Appl Earth Observ and Geoinf 19: 151-162.

591 Reyers B (2004) Incorporating anthropogenic threats into evaluations of regional biodiversity and  
592 prioritisation of conservation areas in the Limpopo Province, South Africa. Biol Conserv 118: 521-  
593 531.

594 Rossiter DG, Loza A (2012) Analyzing land cover change with logistic regression in R. University of  
595 Twente, Faculty of Geo-Information Science & Earth Observation (ITC), Enschede (NL).

596 Rowe S (1992) The ecosystem approach to forestland management. Forest Chron 680: 222-224.

597 Sahid IB, Sugau JB (1993) Allelopathic effect of *Lantana camara* and *Chromolaena odorata* on  
598 selected crops. Weed Sci 41: 303 – 308.

599 Scott JM, Heglund PJ, Morrison ML, Haufler JB, Raphael MG, Wall WA, Samson FB (Eds.) (2002)  
600 Predicting Species Occurrences: Issues of Accuracy and Scale. Island Press, Washington, DC.

601 Skole DL, Tucker CJ (1993) Tropical deforestation and habitat fragmentation in the Amazon: satellite  
602 data from 1978 to 1988. Sci 260: 1905-1910.

603 Sohngen B, Alig R (2000) Mitigation, Adaptation, and Climate Change: results from Recent Research  
604 on U.S. Timber markets. Envir Sci Pol 3:235-248.

605 Suarez AV, Bolger DT, Case TJ (1998) Effects of fragmentation and invasion on native ant  
606 communities in coastal southern California. Ecol 79: 2041-2056.

607 Swets JA, Dawes RM, Monahan J (2000) Better decisions through science. Scient American 283: 82-  
608 87.

609 Turner W, Spector S, Gardiner N, Fladeland M, Sterliug E (2003) Remote sensing of biodiversity  
610 science and conservation. Trends in Ecol & Evol 18: 306-314.

- 611 Underwood E, Ustin S, DiPietro D (2003) Mapping non-native plants using hyperspectral imagery.  
612 Rem Sens of Envir 86: 150-161.
- 613 Underwood E, Ustin S, DiPietro D (2003) Mapping non-native plants using hyperspectral imagery.  
614 Rem Sens of Envir 86: 150-161.
- 615 Ustin SL, Gitelson AA, Jacquemoud S, Schaepman M, Asner GP, Gamon JA (2009) Retrieval of  
616 foliar information about plant pigment systems from high resolution spectroscopy. Rem Sens of  
617 Envir 113: (Supplement 1): S67-S77.
- 618 Václavík T, Meentemeyer R (2009) Invasive species distribution modeling (iSDM): Are absence data  
619 and dispersal constraints needed to predict actual distributions? Ecol Model 220: 3248-3258.
- 620 Van Gils H, Mwanangi M, Rugege D (2006) Invasion of an alien shrub across four land management  
621 regimes, west of St Lucia, South Africa. S Afr J of Sci 102: February.
- 622 Verstraete MM, Pinty B (1996) Designing optimal spectral indexes for remote sensing applications.  
623 IEEE Trans on Geosci and Rem Sens 34: 1254-1265.
- 624 Whitmore TC (1989) Canopy gaps and the two major groups of forest trees. Special feature – Treefall  
625 gaps and forest dynamics. Ecol 70: 536–538.
- 626 Witkowski ETF, Wilson M (2001) Changes in density, biomass, seed banks and seed production of  
627 the alien invasive plant *Chromolaena odorata*, along a 15 year chronosequence. Plant Ecol 152:  
628 13-27.
- 629 World Wildlife Fund (2013). [www.wwf.org](http://www.wwf.org) . Accessed on the 12 December 2013.
- 630 Yang X, Skidmore AK, Melick DR, Shou Z, Xu J (2006) Mapping non-wood forest product  
631 (matsutake mushrooms) using logistic regression and GIS expert system. Ecol Model 198: 208-  
632 218.